



This discussion paper is/has been under review for the journal Atmospheric Chemistry and Physics (ACP). Please refer to the corresponding final paper in ACP if available.

The role of carbonyl sulphide as a source of stratospheric sulphate aerosol and its impact on climate

C. Brühl¹, J. Lelieveld^{1,3}, P. J. Crutzen¹, and H. Tost²

¹Atmospheric Chemistry Department, Max-Planck-Institute for Chemistry, Mainz, Germany

²Institute for Physics of the Atmosphere, Johannes Gutenberg University, Mainz, Germany

³The Cyprus Institute, Nicosia, Cyprus, and King Saud University, Riyadh, Saudi Arabia

Received: 9 June 2011 – Accepted: 18 July 2011 – Published: 22 July 2011

Correspondence to: C. Brühl (christoph.bruehl@mpic.de)

Published by Copernicus Publications on behalf of the European Geosciences Union.

[Title Page](#)

[Abstract](#)

[Introduction](#)

[Conclusions](#)

[References](#)

[Tables](#)

[Figures](#)

[◀](#)

[▶](#)

[◀](#)

[▶](#)

[Back](#)

[Close](#)

[Full Screen / Esc](#)

[Printer-friendly Version](#)

[Interactive Discussion](#)



Abstract

Globally, carbonyl sulphide (COS) is the most abundant sulphur gas in the atmosphere. Our chemistry-climate model of the lower and middle atmosphere with aerosol module realistically simulates the background stratospheric sulphur cycle, as observed by satellites in volcanically quiescent periods. The model results indicate that upward transport of COS from the troposphere largely controls the sulphur budget and the aerosol loading of the background stratosphere. This differs from most previous studies which indicated that short-lived sulphur gases are also important. The model realistically simulates the modulation of the particulate and gaseous sulphur abundance in the stratosphere by the quasi-biennial oscillation (QBO). In the lowermost stratosphere organic carbon aerosol contributes significantly to extinction. Further, we compute that the radiative forcing efficiency by 1 kg of COS is 724 times that of 1 kg CO₂, which translates into an overall radiative forcing by anthropogenic COS of 0.003 W m⁻². The global warming potentials of COS over time horizons of 20 and 100 yr are GWP(20 yr) = 97 and GWP(100 yr) = 27, respectively (by mass). Furthermore, stratospheric aerosol particles produced by the photolysis of COS contribute to a negative radiative forcing, which amounts to -0.007 W m⁻² at the top of the atmosphere for the anthropogenic fraction, more than two times the warming forcing of COS. Considering that the lifetime of COS is twice that of stratospheric aerosols the warming and cooling tendencies approximately cancel. If the forcing of the troposphere near the tropopause is considered, the cooling dominates.

1 Introduction

The anthropogenic increase of greenhouse gases causes a radiative forcing of climate of more than 3 W m⁻² (IPCC, 2007). Conversely, aerosol particles backscatter solar radiation and their anthropogenic emissions exert a global mean negative radiative forcing of about -0.5 W m⁻², being enhanced by a factor of two or more by indirect effects

ACPD

11, 20823–20854, 2011

COS and stratospheric aerosol

Brühl et al.

[Title Page](#)

[Abstract](#)

[Introduction](#)

[Conclusions](#)

[References](#)

[Tables](#)

[Figures](#)

[◀](#)

[▶](#)

[◀](#)

[▶](#)

[Back](#)

[Close](#)

[Full Screen / Esc](#)

[Printer-friendly Version](#)

[Interactive Discussion](#)



COS and stratospheric aerosol

Brühl et al.

[Title Page](#)[Abstract](#)[Introduction](#)[Conclusions](#)[References](#)[Tables](#)[Figures](#)[|◀](#)[▶|](#)[◀](#)[▶](#)[Back](#)[Close](#)[Full Screen / Esc](#)[Printer-friendly Version](#)[Interactive Discussion](#)

the mesosphere, where the most abundant sulphur species is SO_2 (e.g. Rinsland et al., 1995). In the next section we present a brief overview of available information about atmospheric COS, including sources, the chemical behaviour and atmospheric lifetime, while we refer to the more comprehensive review by SPARC (2006) for details. In the subsequent sections we present calculations with a chemistry-climate model and compute the global warming potential of COS. We conclude by assessing the role of COS in the stratospheric sulphur budget and the overall climate effects by anthropogenic emissions.

2 Atmospheric budgets

- 10 Sulphur is an essential trace element for life on Earth, and its availability in the natural environment is usually not rate-limiting for the growth of organisms. One reason is that sulphur is plentiful in seawater. Sulphate is the third abundant compound in sea salt with a mass fraction of about 7.7 %. Moreover, seawater is usually supersaturated with sulphur containing gases. Also in natural terrestrial ecosystems, for example tropical rainforests, sulphur is usually not growth limiting owing to the atmospheric transport from the marine environment. It seems likely that COS may actually play a key role in “nourishing” the natural terrestrial biosphere with sulphur.
- 15

Biological processes produce a range of reduced-sulphur gases (Andreae, 1990). The six most important are H_2S , CS_2 , COS, CH_3SH (methyl mercaptan), CH_3SCH_3 (DMS) and DMDS (dimethyl disulphide). Saline ecosystems such as salt marshes and estuaries are particularly strong sources. The supersaturation of sulphur gases in the aqueous phase relative to the overlying air is largely caused by the microbial degradation of organic matter. Carbon disulphide is not very soluble and seawater is generally supersaturated, so that the oceans are a CS_2 source to the atmosphere. Unfortunately, in situ observations both in the atmosphere and the upper ocean are scarce. Since ocean-atmosphere fluxes are calculated with models that use the measured concentrations in seawater, the source estimates are rather uncertain. Although oceans

[Title Page](#)[Abstract](#)[Introduction](#)[Conclusions](#)[References](#)[Tables](#)[Figures](#)[◀](#)[▶](#)[◀](#)[▶](#)[Back](#)[Close](#)[Full Screen / Esc](#)[Printer-friendly Version](#)[Interactive Discussion](#)

and coastal regions represent the major source of CS_2 , anoxic soils and wetlands can also release significant quantities.

The data availability for COS is somewhat better, but also for this gas the source estimates are associated with substantial uncertainty. The emission categories of COS much resemble those of CS_2 although several additional sources need to be accounted for. For example, it has been observed that rainwater is supersaturated with COS so that outgassing may be significant. The analysis of rain and snow samples has shown that COS is produced photochemically in precipitation (Mu et al., 2004). Further, the burning of biomass releases COS, as observed in the exhaust plumes from boreal and savannah fires (Crutzen et al., 1979). Note that biomass burning is mostly anthropogenic and only a small fraction of the fires is ignited naturally by lightning.

The oceans near the surface are generally COS supersaturated and thus release the gas to the atmosphere, mostly as a function of the temperature-dependent hydrolysis in seawater (Kettle et al., 2002). The flux of COS is therefore highest in high latitudes during summer, whereas in low latitudes the upper ocean can be undersaturated and act as a small sink. The atmospheric oxidation of reduced sulphur gases, in particular DMS and CS_2 , additionally produces COS. Since oceans are an important source of DMS, they are also an indirect source of COS.

By considering the total sulphur source to the atmosphere it becomes evident that in the era of fossil fuel use and industrialization the anthropogenic emission of SO_2 has become a dominant factor in the atmospheric sulphur cycle (Lelieveld et al., 1997). The analysis of an Antarctic ice core has provided evidence that also COS has increased by anthropogenic activity (Montzka et al., 2004). Although atmospheric COS has been rather constant at 450–500 pptv in the past century, its mixing ratio has substantially increased by about 35–40 % from approximately 350 pptv or less since pre-industrial times (Sturges et al., 2001; Montzka et al., 2004; Aydin et al., 2008).

The global atmospheric COS budget has been estimated in Table 1, after Watts (2000). The budget is not balanced though well within the uncertainty ranges, as also concluded by Kettle et al. (2002). Notholt et al. (2003) suggested that tropical biomass

[Title Page](#)[Abstract](#)[Introduction](#)[Conclusions](#)[References](#)[Tables](#)[Figures](#)[◀](#)[▶](#)[◀](#)[▶](#)[Back](#)[Close](#)[Full Screen / Esc](#)[Printer-friendly Version](#)[Interactive Discussion](#)

COS and stratospheric aerosol

Brühl et al.

[Title Page](#)[Abstract](#)[Introduction](#)[Conclusions](#)[References](#)[Tables](#)[Figures](#)[◀](#)[▶](#)[◀](#)[▶](#)[Back](#)[Close](#)[Full Screen / Esc](#)[Printer-friendly Version](#)[Interactive Discussion](#)

Title Page	
Abstract	Introduction
Conclusions	References
Tables	Figures
◀	▶
◀	▶
Back	Close
Full Screen / Esc	
Printer-friendly Version	
Interactive Discussion	



oxidation as associated with coal-fired furnaces. Although these considerations will remain speculative until improved datasets become available, there are indications that both the source and sink terms of COS are substantially underestimated.

Due to its relatively long total effective lifetime of more than two years (i.e. much longer than other S-compounds), some COS survives the slow transport from the tropical troposphere into the stratosphere where it is converted by photodissociation and reaction with O-atoms into SO₂. The latter is oxidised by OH via SO₃ (Sander et al., 2006) into gaseous sulphuric acid, which binds water vapour and forms acidic aerosol particles, dependent on temperature and humidity. In the upper stratosphere sulphuric acid is present in the gas phase. Its photolysis by visible and UV radiation (Vaida et al., 2003; Hintze et al., 2003; Mills, 2005) causes the mixing ratio of SO₂ to increase with altitude (Rinsland et al., 1995).

3 Chemistry-climate model results

To calculate the global transport fluxes and atmospheric chemistry-climate interactions we make use of computer simulations with the ECHAM5 general circulation model (Roeckner et al., 2006), coupled to the Modular Earth Submodel System (MESSy, Jöckel et al., 2006) Atmospheric Chemistry (EMAC) model. The coupled EMAC model together with the aerosol module GMXe (Pringle et al., 2010) and the chemistry module MECCA (Sander et al., 2005) includes a comprehensive account of tropospheric and stratospheric dynamical, cloud, radiation, multiphase chemistry, emission and deposition processes. The aerosol module GMXe has 4 size modes for soluble and 3 for unsoluble aerosol with lognormal distributions. Compared to Pringle et al. (2010) the mode boundaries were adjusted to larger sizes and the sigma values were reduced to accomodate both stratospheric and tropospheric aerosol, see Table 2. In the module we allow for nucleation, coagulation and evaporation using the sulphuric acid vapor pressure approximation by Vehkamäki et al. (2002). It includes also shrinking of particles, i.e. transfer to smaller modes. Accumulation and coarse mode particles

COS and stratospheric aerosol

Brühl et al.

are slowly transported to the troposphere by sedimentation using a modified Walcek scheme (Benduhn, in preparation) with negligible numerical diffusion. The model also considers downward transport of sulphate by sedimentating solid polar stratospheric cloud particles. Lower boundary conditions for the different aerosol types are as described in Pringle et al. (2010).

We apply the model at T42 resolution, i.e. about 2.8° in latitude and longitude. The vertical grid structure resolves the lower and middle atmosphere with 90 layers from the surface to a top layer centred at 0.01 hPa (Giorgetta et al., 2006). This model configuration was selected because it explicitly represents stratosphere-troposphere interactions and has been extensively tested and documented (Lelieveld et al., 2007; Jöckel et al., 2006). The configuration is also able to generate a self-consistent quasi-biennial oscillation in the tropical stratosphere. For evaluation we also performed a simulation with a superimposed injection of SO_2 corresponding to the distribution of observed Pinatubo aerosol in September 1991. The model correctly simulates the transformation to sulphate aerosol, including its optical properties. The removal of the volcanic aerosol in the first 6 months appears to be somewhat too fast as in earlier studies (e.g. Timmreck et al., 1999) due to sedimentation of coarse particles, showing the limitations of applying the 7 mode aerosol module GMXe in both the troposphere and stratosphere. A paper on these results is in preparation.

Considering that the source and sink terms of COS are rather uncertain, we apply measurements from a global network as surface boundary conditions in the model. Since the year 2000 the National Oceanic and Atmospheric Administration (NOAA) has monitored COS in a global flask sampling programme based on 12 measurement stations, mostly located in background locations on islands and remote continental sites (Montzka et al., 2007). The flasks are filled when the wind is from a pre-defined clean air sector to prevent influences by local pollution sources. The measurements and consequently our model results show that the mean mixing ratio in the northern hemisphere, 470–480 pptv, is slightly lower than in the southern hemisphere, 490 pptv, with little interannual variability. Note that some analyses indicated a slow decrease

[Title Page](#)[Abstract](#)[Introduction](#)[Conclusions](#)[References](#)[Tables](#)[Figures](#)[|◀](#)[▶|](#)[◀](#)[▶](#)[Back](#)[Close](#)[Full Screen / Esc](#)[Printer-friendly Version](#)[Interactive Discussion](#)

of atmospheric COS since the 1980s (Sturges et al., 2001; Rinsland et al., 2002), whereas recent data show a slight upward trend (Montzka et al. (2007), and more recent data on the corresponding website). The slight decrease followed by an increase is also seen in Space Shuttle and satellite data of the subtropical lower stratosphere (Rinsland et al., 2008). The annual mean COS mixing ratios in background locations typically vary within 0.48–0.4 ppbv. The highest mean values occur in low latitudes. At middle and low latitudes in the Southern Hemisphere the mixing ratios are slightly lower, whereas the lowest mean levels occur in the Northern Hemisphere.

Our model calculates a global air mass flux across the tropical tropopause (at 100 hPa) of $2.78 \times 10^8 \text{ Mt yr}^{-1}$. Based on a mean COS mixing ratio of 0.485 ppbv at this altitude (Fig. 1) this translates into a mass flux into the stratosphere of 0.15 Mt Syr^{-1} , comparable to previous estimates of the total sulphur flux (SPARC, 2006). The model results demonstrate that during boreal winter the upward transport predominantly occurs south of the equator, to a large extent over the western Pacific. In summer upward fluxes are also rather strong over the western Pacific north of the equator and over the Asian monsoon. If Southeast Asia would be a significant source of CS_2 and COS, this could directly impact the COS flux into the stratosphere through rapid upward transport in the monsoon. Notholt et al. (2003) measured enhanced COS concentrations in the tropical upper troposphere, which they attributed to tropical biomass burning. Direct 15 and seasonal COS measurements over the Tibetan Plateau, where the upward fluxes reach a maximum, and at the tropical tropopause in other locations would provide the information needed to establish if enhanced COS affects the stratosphere and thus help test our model results.

Figure 1 presents model calculated zonal mean COS mixing ratios for two selected 20 months at equinox for different phases of the quasi-biennial oscillation. COS is most abundant in the tropics and has a significant seasonal variability, being most pronounced in the northern hemisphere. Consistent with observations, the model results show relatively high COS mixing ratios in the tropics at the surface while they extend up to about 16 km altitude near the tropopause. Notholt et al. (2003) observed COS mixing

Title Page	
Abstract	Introduction
Conclusions	References
Tables	Figures
◀ ▶	
◀	▶
Back	Close
Full Screen / Esc	

Printer-friendly Version
Interactive Discussion



COS and stratospheric aerosol

Brühl et al.

ratios in excess of 0.5 ppbv between 8 and 16 km altitude, though their measurements were limited to the Atlantic Ocean and to relatively short periods during and after the biomass burning season. If the measurements of Notholt et al. would be representative for the entire year and globe, we would underestimate COS at the tropical tropopause and its transport into the stratosphere by about 20–25 %. However, the evidence for an upper tropospheric COS maximum is mixed, only partly corroborated by Space Shuttle measurements in the 1990s (SPARC, 2006). Moreover, measurements over the Pacific Ocean at 10–12 km altitude give no evidence of enhanced COS (Blake et al., 2004). Recent satellite observations by ACE-FTS show up to about 0.48 ppbv COS near the tropopause (Barkley et al., 2008), which corroborates our model simulations (Fig. 1) based on the observed surface concentrations. The model also reproduces the modulation by the QBO leading to interannual variability of the the stratospheric sulphur source.

Figure 2 shows the production of anorganic sulphur from COS, indicating that photolysis is dominating. In the absense of sinks it would take about 1 yr to reach the observed sulphate concentrations. In our simulations where stratospheric mixing ratios of SO_2 , gaseous H_2SO_4 and sulphate aerosol were initialized from zero and the ones of COS with the observed distributions (January 1996), most of the stratospheric aerosol layer formed in the first year. It takes about 3 yr to reproduce also the gaseous anorganic sulphur species in the middle and upper stratosphere close to observations due to the long transport times. In Fig. 3 it is illustrated that the sharp vertical gradient of COS in the stratosphere coincides with a sharp increase of particulate sulphuric acid with altitude (cf. Fig. 1). Figure 4, for another season and QBO phase, shows large differences in the distribution of sulphate to Fig. 3 in the tropics but again good agreement of the patterns with observations. Sulphate from COS appears to account for about 65 to 75 % of the observed aerosol as derived from SAGE observations (e.g. Thomason et al., 1997). In the lower stratosphere organic carbon aerosol appears to contribute significantly to aerosol surface area density and mixing ratios. Figure 5 shows the temporal evolution of simulated sulphate aerosol in the tropics after 3 yr of

[Title Page](#)[Abstract](#)[Introduction](#)[Conclusions](#)[References](#)[Tables](#)[Figures](#)[|◀](#)[▶|](#)[◀](#)[▶](#)[Back](#)[Close](#)[Full Screen / Esc](#)[Printer-friendly Version](#)[Interactive Discussion](#)

spinup, modulated by the QBO (black contours) together aerosol mixing ratios derived from SAGE data (without extrapolations for data gaps) using the empirical formula by Grainger et al. (1995). Our model results, which yield a maximum sulphate mixing ratio of 0.35 ppb in the tropics, agree well with satellite measurements (SAGE), including the modulation by the QBO. Sulphate aerosol thus explains on average 70 % of the observations. This is within the uncertainty introduced by conversion of extinction and aerosol surface density to volume mixing ratios. The model results indicate that dust and especially organic carbon aerosol also contribute to the aerosol in the lowermost stratosphere as also mentioned in the SAGE evaluation by Thomason et al. (2008) and in the compilation of in situ observations by Murphy et al. (2007). Including organic carbon reproduces most of the seasonal patterns observed by SAGE in the lower stratosphere (Fig. 5).

As shown in Figure 6, above about 10 hPa (about 30 km) or a temperature of 233 K most of the simulated sulphur is in the gas phase. In the middle stratosphere H_2SO_4 vapor is most abundant. Near the stratopause (and higher up) SO_2 is the dominating species with about 1 ppbv as observed by ATMOS (Rinsland et al., 1995).

The calculated extinction of the total aerosol at 1000 nm in Fig. 7 also agrees well and consistently (i.e. low by about 35 %) with observations of SAGE (SPARC, 2006). This holds also for extinction at 530 nm (not shown). The dominating contributions to total extinction are sulphate, aerosol water and organic carbon as shown in Fig. 8. Dust contributes in the upper northern tropical troposphere. The calculated extinction at 2450 nm is about 60 % low compared to HALOE in the Junge layer which might be due to the setup of the Mie lookup tables which are optimized for shorter wavelengths. Figure 7 furthermore suggests that our model underestimates aerosol extinction in the upper stratosphere. It is conceivable that an assumed flux of meteoric dust of about 0.01–0.02 Mt yr⁻¹ (SPARC, 2006) would reduce the "missing" aerosol source by about half in the lower and middle stratosphere.

In the model of Weisenstein et al. (1997), which was also used by SPARC (2006), SO_2 mixing ratios of 40–50 ppt were prescribed in air transported into the stratosphere.

[Title Page](#)[Abstract](#)[Introduction](#)[Conclusions](#)[References](#)[Tables](#)[Figures](#)[|◀](#)[▶|](#)[◀](#)[▶](#)[Back](#)[Close](#)[Full Screen / Esc](#)[Printer-friendly Version](#)[Interactive Discussion](#)

Furthermore additional small fluxes of other short-lived gases such as CS₂ and H₂S were included. This seems at odds with measured SO₂ mixing ratios in the background upper troposphere, which are generally below 10–20 ppt (Thornton et al., 1999). In fact, upward transport through the tropical tropopause layer (12–18 km altitude) is very slow and the air mass residence time is several months. The chemical lifetime of SO₂ through reaction with OH in the tropical tropopause layer is about two weeks and that of CS₂, H₂S and DMS only a few days. Therefore it seems unlikely that short-lived sulphur gases could survive oxidation into H₂SO₄ and be transported into the stratosphere. Furthermore, H₂SO₄ has a low volatility and quickly deposits onto the surfaces of ice crystals, ubiquitously present in the tropical tropopause layer. Since less than 1 % of the water that enters the tropopause layer at 12 km actually reaches the stratosphere at 18 km, associated with the “freeze-drying” of the cold tropopause, most water is removed by the sedimentation of ice particles, which also prevents sulphuric acid to reach the stratosphere. Our results are thus consistent with the hypothesis of Crutzen (1976) that the stratospheric sulphate layer in volcanically quiescent periods is controlled by the oxidation of COS, at least for about 70 %.

4 Climate effects and GWP

Some trace constituents in the atmosphere, in particular halocarbons and COS, have infrared (IR) absorption bands in the 8–14 µm wavelength region, the atmospheric window, and as a consequence they can efficiently enhance the greenhouse effect. Gases such as CO₂ and water vapour absorb at longer IR wavelengths, so that 60–80 % of the radiation emitted in the window region passes the atmosphere unattenuated. In fact, molecules with bonds between carbon, fluorine and sulphur are particularly efficient in absorbing this IR radiation, so that their increase contributes to heating of our planet. Overall, the efficiency of greenhouse warming of a molecule depends on the strength of its IR absorption bands as well as its concentration, the latter being determined by the sources and the atmospheric lifetime. To account for both the radiative forcing of a

[Title Page](#)
[Abstract](#) [Introduction](#)
[Conclusions](#) [References](#)
[Tables](#) [Figures](#)

[◀](#) [▶](#)
[◀](#) [▶](#)
[Back](#) [Close](#)
[Full Screen / Esc](#)

[Printer-friendly Version](#)
[Interactive Discussion](#)



molecule and its long-term climate impact the concept of the global warming potential (GWP) has been developed, a metric that has been used in the Kyoto Protocol. The GWP is based on the time-integrated global mean radiative forcing of a pulse emission of a compound relative to that of the reference gas CO₂. Here we present the GWP on a mass/mass basis for the time horizons Δt of 20 and 100 yr, approximated by the following expression (Roehl et al., 1995): $GWP_{\Delta t} = \frac{RF_{\text{COS}}}{RF_{\text{CO}_2}} \frac{\tau_{\text{COS}}}{\tau_{\text{CO}_2}} \frac{1-e^{-\Delta t/\tau_{\text{COS}}}}{1-e^{-\Delta t/\tau_{\text{CO}_2}}}$. This mass-based GWP can be converted into the mole-based GWP by multiplying with the ratio of the molecular weights. The steady state GWP is calculated for Δt → ∞, whereby the last term on the rhs approaches 1. For the lifetime of COS we adopt τ_{COS} = 2 yr, while for τ_{CO₂} a sum of exponential terms is applied, as recommended by the IPCC, leading to an effective lifetime of τ_{CO₂} ≈ 75 yr for a time horizon of Δt = 100 yr. For the first term on the rhs, the radiative forcing (RF) of 1 kg of COS relative to 1 kg of CO₂ added to the present atmosphere, we compute a value of 724. This means that COS is 724 times more efficient in perturbing the energy balance of the atmosphere than CO₂. By inserting the above mentioned lifetimes we obtain a GWP of COS of 97 for Δt = 20 yr, and of 27 for Δt = 100 yr (note that this translates into molar GWPs of 132 and 36 for time horizons of Δt = 20 and 100 yr, respectively). By using the information from ice cores about the natural atmospheric mixing ratio of COS, being 70 % of the present level, we calculate that the human-induced enhancement of COS exerts a radiative forcing of about 0.003 W m⁻². As discussed above, the uptake by the biosphere limits the lifetime of COS in the atmosphere. Based on the chemical lifetime alone (35 yr) the GWP would be nearly 17 times higher for a time horizon of Δt = 100. Of course, the biosphere-controlled lifetime also limits transport to the stratosphere where COS also exerts a radiative forcing. The stratospheric breakdown of COS into SO₂ and sulphuric acid is followed by the formation of aerosol particles that grow by the continued deposition of H₂SO₄ and coagulation. The latter process levels off at a steady state effective particle radius (i.e. surface area weighted) of approximately 0.3 μm (SPARC, 2006), also because of sedimentation. Particles of this size effectively interact with solar radiation, also because the solar spectrum has an energy maximum at a wavelength of

[Title Page](#)[Abstract](#)[Introduction](#)[Conclusions](#)[References](#)[Tables](#)[Figures](#)[◀](#)[▶](#)[◀](#)[▶](#)[Back](#)[Close](#)[Full Screen / Esc](#)[Printer-friendly Version](#)[Interactive Discussion](#)

Title Page

Abstract

Introduction

Conclusions

References

Tables

Figures

1

▶

▶

Back

Close

Full Screen / Esc

[Printer-friendly Version](#)

Interactive Discussion



exerts a negative radiative forcing of about -0.007 W m^{-2} , which actually exceeds the positive forcing of COS by more than a factor of two. Since the e-folding lifetime of stratospheric aerosol is about one year (thus half of τ_{COS}) the global “cooling” potential of COS through stratospheric aerosol formation is equivalent to the above derived GWP. Therefore, if we account for indirect effects in GWP calculations, also customary for gases such as methane (IPCC, 2007), it follows that COS has no net climate impact. This also applies to the precursor gas CS_2 , which has a very short lifetime and an insignificant GWP.

The average forcing by stratospheric background aerosol at 185hPa (about the tropopause) is -0.09 W m^{-2} . A large fraction of that is due to organic carbon aerosol (including black carbon) near the tropical tropopause. Figure 9 shows that this forcing is strongly influenced by the large local variability due to clouds and surface albedo. The largest negative forcing is in subtropical regions with clear skies and a low surface albedo, i.e. over the oceans.

15 5 Conclusions

Carbonyl sulphide, an efficient greenhouse gas, is the most abundant sulphur gas in the atmosphere. Its anthropogenic emissions and that of CS_2 , the latter being converted into COS, contribute approximately 30 % to the global COS mixing ratio of about 0.5 ppbv. By applying surface measurements of COS from a global network of 12 stations as boundary conditions, our chemistry-climate model reproduces the atmospheric COS cycle well. The observational database for COS, CS_2 and SO_2 , especially for the tropical tropopause layer (12–18 km altitude), is presently insufficient for a conclusive evaluation of the sulphur cycle and associated aerosol production in the background stratosphere, i.e. during volcanically quiescent periods. Nevertheless, we present compelling evidence that COS plays a controlling role, as stated by Crutzen (1976). Our model results indicate that the COS controlled sulphur flux into the stratosphere is $0.15 \text{ Mt S yr}^{-1}$, whereas in previous evaluations the same flux

[Title Page](#)
[Abstract](#) [Introduction](#)
[Conclusions](#) [References](#)
[Tables](#) [Figures](#)

[◀](#) [▶](#)
[◀](#) [▶](#)
[Back](#) [Close](#)
[Full Screen / Esc](#)

[Printer-friendly Version](#)
[Interactive Discussion](#)



COS and
stratospheric aerosol

Brühl et al.

[Title Page](#)[Abstract](#)[Introduction](#)[Conclusions](#)[References](#)[Tables](#)[Figures](#)[|◀](#)[▶|](#)[◀](#)[▶](#)[Back](#)[Close](#)[Full Screen / Esc](#)[Printer-friendly Version](#)[Interactive Discussion](#)

of S was obtained, including the assumed direct transport of SO₂, CS₂ and H₂S across the tropical tropopause. We consider the latter assumption to be unlikely and not needed to explain observations of the background stratospheric aerosol. Our chemistry climate model with aerosol module is able to reproduce most of the features observed by SAGE, including the modulation of stratospheric aerosol by the QBO and the seasonal effects. It also reproduces SO₂ in the upper stratosphere observed by ATMOS on the Space Shuttle. We compute the climate effects and the global warming potential (GWP) of COS, which accounts for the radiative forcing as well as the atmospheric lifetime. The radiative forcing by 1 kg of COS, i.e. the enhancement of the greenhouse effect, is 724 times that of 1 kg CO₂. Based on a 30 % contribution of human-induced emissions to COS in the present atmosphere, the IR radiative forcing of COS is 0.003 W m⁻². The GWP of COS over time horizons of 20 and 100 years is GWP(20 yr) = 97 and GWP(100 yr) = 27, respectively. However, through its contribution to stratospheric aerosols COS also exerts a radiative cooling forcing, which amounts to about -0.007 W m⁻², more than twice the warming forcing. Since the atmospheric lifetime of COS is about 2 yr and the COS-derived aerosol lifetime only 1 yr, the opposing climate effects tend to cancel and the net GWP of COS is insignificant. This also applies to CS₂ in view of its very short atmospheric lifetime of a few days and its partial conversion to COS.

The service charges for this open access publication have been covered by the Max Planck Society.

Acknowledgements. We thank Kirsty Pringle of the University of Leeds, UK, who contributed significantly to the development of the aerosol module. Also we thank our colleagues of MPI for Chemistry, Mainz, Germany, Francois Benduhn for providing his yet unpublished sedimentation scheme and Swen Metzger for the aerosol thermodynamics scheme EQSAM. We further thank Lamont Poole and Larry Thomason of NASA Langley Research Center, Hampton, USA, for their advice on SAGE data. We acknowledge the European Research Council for support of the C8 project.

References

- Andreae, M. O.: Ocean-atmosphere interactions in the global biogeochemical sulphur cycle, *Marine Chem.*, 30, 1–29, 1990.
- Aydin, M., Williams, M. B., Tatum, C., and Saltzman, E. S.: Carbonyl sulfide in air extracted from a South Pole ice core: a 2000 year record, *Atmos. Chem. Phys.*, 8, 7533–7542, doi:10.5194/acp-8-7533-2008, 2008.
- Bandy, A. R., Thornton, D. C., Scott, D. L., Lalevic, M., Lewis, E. E., and Driedger III, A. R.: A time series for carbonyl sulfide in the Northern Hemisphere, *J. Atmos. Chem.*, 14, 527–534, 1992. 20826
- Barkley, M. P., Palmer, P. I., Boone, C. D., Bernath, P. F., and Suntharalingam, P.: Global distributions of carbonyl sulfide in the upper troposphere and stratosphere, *Geoph. Res. Lett.*, 35, L14810, doi:10.1029/2008GL034270, 2008. 20827
20825
- Blake, N.J., Streets, D. G., Woo, J.-H., Simpson, I. J., Green, J., Meinardi, S., Kita, K., Atlas, E., Fuelberg, H. E., Sachse, G., Avery, M. A., Vay, S. A., Talbot, R. W., Dibb, J. E., Bandy, A. R., Thornton, D. C., Rowland, F. S., and Blake, D. R.: Carbonyl sulfide and carbon disulfide: Large-scale distributions over the western Pacific and emissions from Asia during TRACE-P, *J. Geophys. Res.*, 109, D15S05, doi:10.1029/2003JD004259, 2004. 20825, 20832, 20846
20832
- Campbell, J. E., Carmichael, G. R., Chai, T., Mena-Carrasco, M., Tang, Y., Blake, D. R., Blake, N. J., Vay, S. A., Collatz, G. J., Baker, I., Berry, J. A., Montzka, S. A., Sweeney, C., Schnoor, J. L., and Stanier, C. O.: Photosynthetic control of atmospheric carbonyl sulfide during the growing season, *Science*, 322, 1085–1088, 2008. 20828
- Crutzen, P. J.: The possible importance of CSO for the sulphate layer of the stratosphere, *Geophys. Res. Lett.*, 3, 73–76, 1976. 20825, 20834, 20837
- Crutzen, P. J., Heidt, L. E., Krasnec, J. P., Pollock, W. H., and Seiler, W.: Biomass burning as a source of atmospheric gases: CO, H₂, N₂O, NO, CH₃Cl, and COS, *Nature*, 282, 253–256, 1979. 20827
- Giorgetta, M. A., Manzini, E., Roeckner, E., Esch, M., and Bengtsson, L.: Climatology and forcing of the quasi-biennial oscillation in the MAECHAM5 model, *J. Climate*, 19, 3882–3901, 2006. 20830

ACPD

11, 20823–20854, 2011

COS and
stratospheric aerosol

Brühl et al.

[Title Page](#)

[Abstract](#)

[Introduction](#)

[Conclusions](#)

[References](#)

[Tables](#)

[Figures](#)

◀

▶

◀

▶

[Back](#)

[Close](#)

[Full Screen / Esc](#)

[Printer-friendly Version](#)

[Interactive Discussion](#)



Grainger, R. G., Lambert, A., Rodgers, C. D., Taylor, F. W., and Deshler, T.: Stratospheric aerosol effective radius, surface area and volume estimated from infrared measurements, *J. Geophys. Res.*, 100, 16507–16518, 1995. 20833

Hintze, P. E., Kjaergaard, H. G., Vaida, V., and Burkholder, J. B.: Vibrational and electronic spectroscopy of sulfuric acid vapor, *J. Phys. Chem. A*, 107, 1112–1118, 2003. 20829

5 Intergovernmental Panel on Climate Change (IPCC), *Climate Change 2007: The Physical Science Basis*, edited by: Solomon, S., Qin, D., Manning, M., Chen, Z., Marquis, M., Averyt, K. B., Tignor, M., and Miller, H. L., Cambridge University Press, Cambridge, UK, and New York, NY, USA, 2007. 20824, 20825, 20837

10 Jöckel, P., Tost, H., Pozzer, A., Brühl, C., Buchholz, J., Ganzeveld, L., Hoor, P., Kerkweg, A., Lawrence, M. G., Sander, R., Steil, B., Stiller, G., Tanarhte, M., Taraborelli, D., van Aardenne, J., and Lelieveld, J.: The atmospheric chemistry general circulation model ECHAM5/MESSy: Consistent simulation of ozone from the surface to the mesosphere, *Atmos. Chem. Phys.*, 6, 5067–5104, doi:10.5194/acp-6-5067-2006, 2006. 20829, 20830

15 Junge, C. E., Chagnon, C. W., and Manson, J. E.: Stratospheric aerosols, *J. Meteorol.*, 18, 81–108, 1961. 20825

Kettle, A. J., Kuhn, U., von Hobe, M., Kesselmeier, J., and Andreae, M. O.: Global budget of atmospheric carbonyl sulphide: Temporal and spatial variations of the dominant sources and sinks, *J. Geophys. Res.*, 107, 4658, doi:10.1029/2002JD002187, 2002. 20827, 20828

20 Kuhn, U., Ammann, C., Wolf, A., Meixner, F. X., Andreae, M. O., and Kesselmeier, J.: Carbonyl sulphide exchange on an ecosystem scale: soil represents a dominant sink for atmospheric COS, *Atmos. Environ.*, 33, 995–1008, 1999. 20828

Lelieveld, J., Roelofs, G. J., Ganzeveld, L., Feichter, J., and Rodhe, H.: Terrestrial sources and distribution of atmospheric sulphur, *Phil. Trans. R. Soc. London, B*, 352, 149–158, 1997. 25 20827

Lelieveld, J., Brühl, C., Jöckel, P., Steil, B., Crutzen, P. J., Fischer, H., Giorgetta, M. A., Hoor, P., Lawrence, M. G., Sausen, R., and Tost, H.: Stratospheric dryness: model simulations and satellite observations, *Atmos. Chem. Phys.*, 7, 1313–1332, doi:10.5194/acp-7-1313-2007, 2007. 20830

30 McCormick, M. P., Thomason, L. W., and Trepte, C. R.: Atmospheric effects of the Mt Pinatubo eruption, *Nature*, 373, 399–404, 1995. 20825, 20836

Minnis, P., Harrison, E. F., Stowe, L. L., Gibson, G. G., Denn, F. M., Doelling, D. R., and Smith, Jr., W. L.: Radiative climate forcing by the Mount Pinatubo eruption, *Science*, 259,

Title Page

Abstract

Introduction

Conclusions

References

Tables

Figures

◀

▶

◀

▶

Back

Close

Full Screen / Esc

Printer-friendly Version

Interactive Discussion



- Mihalopoulos, N., Putaud, J. P., Nguyen, B. C., and Belviso, S.: Annual variation of atmospheric carbonyl sulfide in the marine atmosphere in the southern Indian Ocean, *J. Atmos. Chem.*, 13, 73–82, 1991. 20825
- 5 Mills, M. J., Toon, O. B., and Thomas, G. E.: Mesospheric sulfate aerosol layer, *J. Geophys. Res.*, 110, D24208, doi:10.1029/2005JD006242, 2005. 20829
- Montzka, S. A., Aydin, M., Battle, M., Butler, J. H., Saltzman, E. S., Hall, B. D., Clarke, A. D., Mondeel, D., and Elkins, J. W.: A 350-year atmospheric history for carbonyl sulfide inferred from Antarctic firn air and air trapped in ice, *J. Geophys. Res.*, 109, D22302, doi:10.1029/2004JD004686, 2004. 20827, 20836
- 10 Montzka, S. A., Calvert, P., Hall, B. D., Elkins, J. W., Conway, T. J., Tans, P. P., and Sweeney, C.: On the global distribution, seasonality, and budget of atmospheric carbonyl sulfide and some similarities with CO₂, *J. Geophys. Res.*, 112, D09302, doi:10.1029/2006JD007665, 2007. 20825, 20830, 20831
- 15 Mu, Y., Geng, C., Wang, M., Wu, H., Zhang, X., and Jiang, G.: Photochemical production of carbonyl sulphide in precipitation, *J. Geophys. Res.*, 109, D13301, doi:10.1029/2003JD004206, 2004. 20827
- Murphy, D. M., Cziczo, D. J., Hudson, P. K., and Thomson, D. S.: Carbonaceous material in aerosol particles in the lower stratosphere and tropopause region, *J. Geophys. Res.*, 112, D04203, doi:10.1029/2006JD007297, 2007. 20833
- 20 Notholt, J., Kuang, Z., Rinsland, C. P., Toon, G. C., Rex, M., Jones, N., Albrecht, T., Deckelmann, H., Krieg, J., Weinzierl, C., Bingemer, H., Weller, R., and Schrems, O.: Enhanced upper tropical tropospheric COS: Impact on the stratospheric aerosol layer, *Science*, 300, 307–310, 2003. 20827, 20831
- 25 Pringle, K. J., Tost, H., Metzger, S., Steil, B., Giannadaki, D., Nenes, A., Fountoukis, C., Stier, P., Vignati, E., and Lelieveld, J.: Description and evaluation of GMXe: a new aerosol submodel for global simulations (v1), *Geosci. Model Dev.*, 3, 391–412, 2010. 20829, 20830
- Rinsland, C. P., Gunson, M. R., Ko, M. K. W., Weisenstein, D. W., Zander, R., Abrams, M. C., Goldman, A., Sze, N. D., and Yue, G. K.: H₂SO₄ photolysis: A source of sulfur dioxide in the upper stratosphere, *Geophys. Res. Lett.*, 22, 1109–1112, 1995. 20826, 20829, 20833
- 30 Rinsland, C. P., Goldman, A., Mahieu, E., Zander, R., Notholt, J., Jones, N. B., Griffith, D. W. T., Stephen, T. M., and Chiou, L. S.: Ground-based infrared spectroscopic measurements of carbonyl sulfide: Free tropospheric trends from a 24-year time series of solar

COS and stratospheric aerosol

Brühl et al.

[Title Page](#)[Abstract](#)[Introduction](#)[Conclusions](#)[References](#)[Tables](#)[Figures](#)[◀](#)[▶](#)[◀](#)[▶](#)[Back](#)[Close](#)[Full Screen / Esc](#)[Printer-friendly Version](#)[Interactive Discussion](#)

absorption measurements, *J. Geophys. Res.*, 107(D22), 4657, doi:10.1029/2002JD002522, 2002. 20831

Rinsland, C. P., Chiou, L., Mahieu, E., Zander, R., Boone, C. D., Bernath, P. F.: Measurements of long-term changes in atmospheric OCS (carbonyl sulfide) from infrared solar observations, *J. Quant. Spectrosc. Ra.*, 109, 2679–2686, 2008. 20831

5 Robock, A.: Volcanic eruptions and climate, *Rev. Geophys.*, 38, 191–219, 2000. 20825

Roeckner, E., Brokopf, R., Esch, M., Giorgetta, M., Hagemann, S., Kornblueh, L., Manzini, E., Schlese, U., and Schulzweida, U.: Sensitivity of simulated climate to horizontal and vertical resolution in the ECHAM5 atmosphere model, *J. Climate*, 19, 3771–3791, 2006. 20829

10 Roehl, C. M., Boglu, D., Brühl, C., and Moortgat, G. K.: Infrared band intensities and global warming potentials of CF_4 , C_2F_6 , C_3F_8 , C_4F_{10} , C_5F_{12} , and C_6F_{14} , *Geophys. Res. Lett.*, 22, 815–818, 1995. 20835

15 Sander, R., Kerkweg, A., Jöckel, P., and Lelieveld, J.: Technical note: The new comprehensive atmospheric chemistry module MECCA, *Atmos. Chem. Phys.*, 5, 445–450, doi:10.5194/acp-5-445-2005, 2005. 20829

Sander, S. P., Friedl, R. R., Golden, D. M., Kurylo, M. J., Moortgat, G. K., Keller-Rudek, H., Wine, P. H., Ravishankara, A. R., Kolb, C. E., Molina, M. J., Finlayson-Pitts, B. J., Huie, R. E., and Orkin, V. L.: Chemical Kinetics and Photochemical Data for Use in Atmospheric Studies, Evaluation Number 15, JPL Publication 06-2, Jet Propulsion Laboratory, Pasadena, 2006. 20829

20 Sandoval-Soto, L., Stanimirov, M., von Hobe, M., Schmitt, V., Valdes, J., Wild, A., and Kesselmeier, J.: Global uptake of carbonyl sulfide (COS) by terrestrial vegetation: Estimates corrected by deposition velocities normalized to the uptake of CO_2 , *Biogeosci.*, 2, 125–132, 2005. 20828

25 Stratospheric Processes and their Role in Climate (SPARC), Assessment of Stratospheric Aerosol Particles, edited by: Thomason, L. and Peter, T., SPARC Report No. 4, WMO/WCRP, 2006. 20826, 20831, 20832, 20833, 20835

Steinbacher, M., Bingemer, H. G., and Schmidt, U.: Measurements of the exchange of carbonyl sulfide (OCS) and carbon disulfide (CS_2) between soil and atmosphere in a spruce forest in central Germany, *Atmos. Environ.*, 38, 6043–6052, 2004. 20828

30 Stenchikov, G. L., Kirchner, I., Robock, A., Graf, H.-F., Antuña, J. C., Grainger, R. G., Lambert, A., and Thomason, L.: Radiative forcing from the 1991 Mount Pinatubo volcanic eruption, *J. Geophys. Res.*, 103, 13837–13857, 1998. 20836

Brühl et al.

[Title Page](#)

[Abstract](#)

[Introduction](#)

[Conclusions](#)

[References](#)

[Tables](#)

[Figures](#)

[◀](#)

[▶](#)

[◀](#)

[▶](#)

[Back](#)

[Close](#)

[Full Screen / Esc](#)

[Printer-friendly Version](#)

[Interactive Discussion](#)



- Sturges, W. T., Penkett, S. A., Barnola, J.-M., Chappellaz, J., Atlas, E., and Stroud, V.: A long-term record of carbonyl sulfide (COS) in two hemispheres from firn air measurements, *Geophys. Res. Lett.*, 28, 4095–4098, 2001. 20827, 20831
- Thomason, L. W., Poole, L. R., and Deshler, T.: A global climatology of stratospheric aerosol surface area density deduced from Stratospheric Aerosol and Gas Experiment II measurements: 1984–1994, *J. Geophys. Res.*, 102, 8967–8976, 1997. 20832
- Thomason, L. W., Burton, S. P., Luo, B.-P., and Peter, T.: SAGE II measurements of stratospheric aerosol properties at non-volcanic levels, *Atmos. Chem. Phys.*, 8, 983–995, doi:10.5194/acp-8-983-2008, 2008. 20833
- Thornton, D. C., Bandy, A., Blomquist, B., Driedger, A., and Wade, T.: Sulfur dioxide distributed over the Pacific Ocean 1991–1996, *J. Geophys. Res.*, 104, 5845–5854, doi:10.1029/1998JD100048, 1999. 20834
- Timmreck, C., Graf, H.-F., and Feichter, J.: Simulation of Mt. Pinatubo volcanic aerosol with the Hamburg climate model ECHAM4, *Theor. Appl. Climatol.*, 62, 85–108, 1999. 20830
- Turco, R. P., Whitten, R. C., Toon, O. B., Pollack, J. B., Hamill, P.: OCS, stratospheric aerosols and climate, *Nature*, 283, 283–285, 1980. 20825
- Vaida, V., Kjaergaard, H. G., Hintze, P. E., Donaldson, D. J.: Photolysis of sulfuric acid vapor by visible solar radiation, *Science*, 299, 1566–1568, 2003. 20829
- Van Diest, H. and Kesselmeier, J.: Soil atmosphere exchange of carbonyl sulfide (COS) regulated by diffusivity depending on water-filled pore space, *Biogeosci.*, 5, 475–483, 2008. 20828
- Vehkämäki, H., Kulmala, M., Napari, I., Lehtinen, K. E. J., Timmreck, C., Noppel, M., and Laaksonen, A.: An improved parameterization for sulfuric acid-water nucleation rates for tropospheric and stratospheric conditions, *J. Geophys. Res.*, 107(D22), 4622, doi:10.1029/2002JD002184, 2002. 20829
- Watts, S. F.: The mass budgets of carbonyl sulfide, dimethyl sulfide, carbon disulfide and hydrogen sulfide, *Atmos. Environ.*, 34, 761–779, 2000. 20827, 20828, 20844
- Weisenstein, D. K., Yue, G., Ko, M., Sze, N.-D., Rodriguez, J., and Scott, C.: A two-dimensional model of sulfur species and aerosols, *J. Geophys. Res.*, 102, 13019–13035, doi:10.1029/97JD00901, 1997. 20833

[Title Page](#)[Abstract](#)[Introduction](#)[Conclusions](#)[References](#)[Tables](#)[Figures](#)[◀](#)[▶](#)[◀](#)[▶](#)[Back](#)[Close](#)[Full Screen / Esc](#)[Printer-friendly Version](#)[Interactive Discussion](#)

Table 1. Global atmospheric budget of COS after Watts (2000).

Source/Sink	Annual flux (Mt yr^{-1})
Sources	
Open ocean	0.10 ± 0.15
Coastal ocean (incl. salt marshes, estuaries)	0.20 ± 0.10
Anoxic soils	0.02 ± 0.01
Wetlands	0.03 ± 0.03
Volcanism	0.05 ± 0.04
Precipitation	0.13 ± 0.08
DMS oxidation	0.17 ± 0.04
CS_2 oxidation (50 % anthropogenic)	0.42 ± 0.12
Biomass burning	0.07 ± 0.05
Anthropogenic (direct)	0.12 ± 0.06
Total source	1.31 ± 0.25
Sinks	
Oxic soils	0.92 ± 0.78
Vegetation	0.56 ± 0.10
Reaction with OH	0.13 ± 0.10
Reaction with O	0.02 ± 0.01
Photodissociation	0.03 ± 0.01
Total sink	1.66 ± 0.79
Total imbalance	0.35 ± 0.83

COS and stratospheric aerosol

Brühl et al.

[Title Page](#)[Abstract](#)[Introduction](#)[Conclusions](#)[References](#)[Tables](#)[Figures](#)[◀](#)[▶](#)[◀](#)[▶](#)[Back](#)[Close](#)[Full Screen / Esc](#)[Printer-friendly Version](#)[Interactive Discussion](#)

Table 2. Parameters of the aerosol size distribution in GMXe. Nucleation mode only for soluble particles.

Mode	Nucleation	Aitken	Accumulation	Coarse
$r_{\min}, \mu\text{m}$	0.0005	0.006	0.07	1
σ	1.59	1.59	1.49	1.7

Title Page	
Abstract	Introduction
Conclusions	References
Tables	Figures
Discussion Paper	
 ◀	▶
◀	▶
Back	Close
Full Screen / Esc	
Printer-friendly Version	
Interactive Discussion	



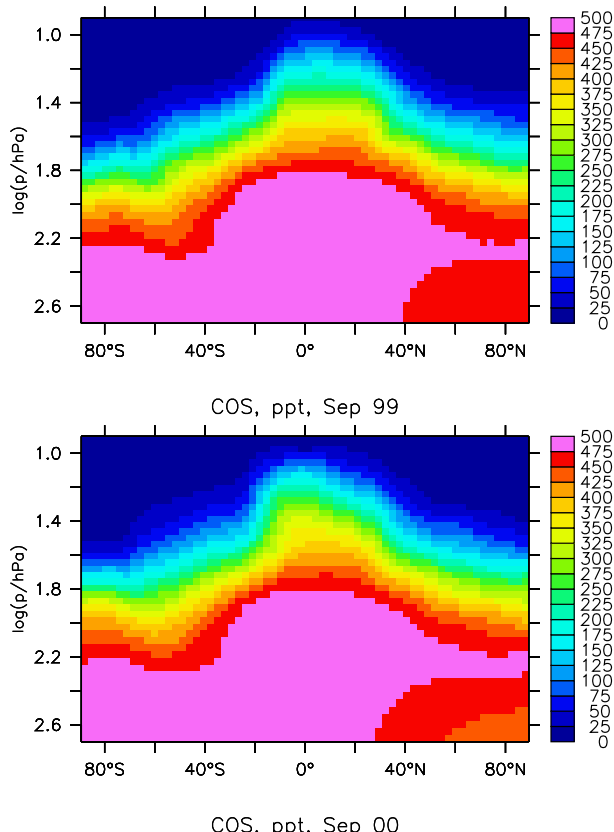


Fig. 1. EMAC model calculated zonal mean COS mixing ratios (in pptv) for September in different QBO phases (1999 and 2000). Color scale as in Barkley et al. (2008).

COS and stratospheric aerosol

Brühl et al.

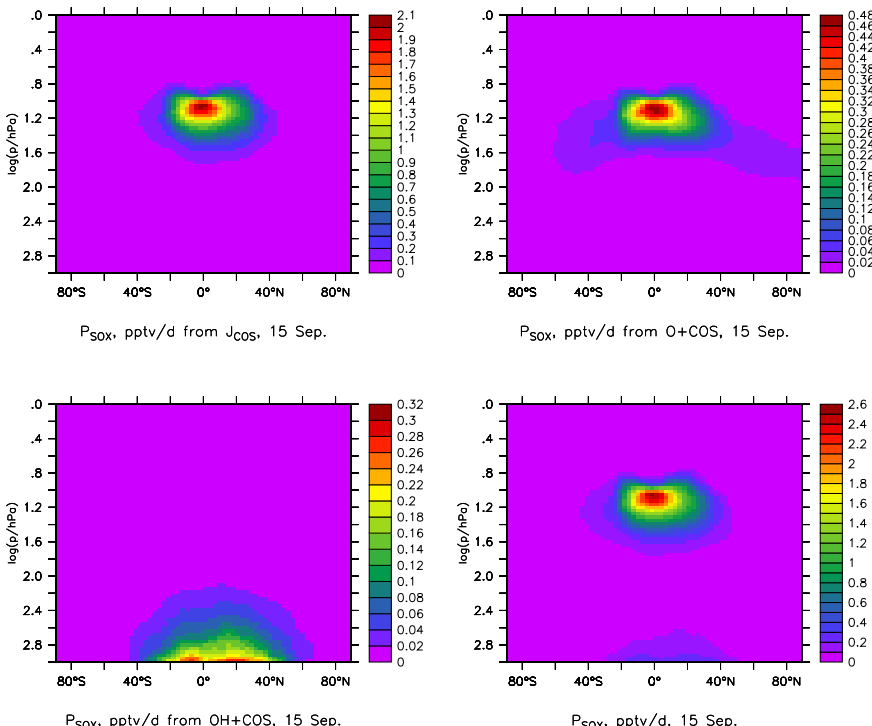


Fig. 2. SO_x production from COS, pptv day⁻¹, September 2000. Upper left: photolysis, upper right: reaction with O(³P), lower left: reaction with OH, lower right: total.

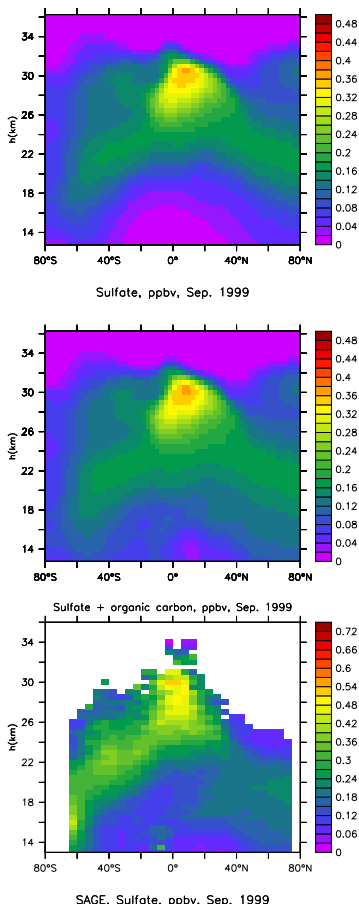


Fig. 3. Simulated (upper panel) and observed (lower panel, derived from SAGE) sulphate aerosol in September 1999, ppbv. The middle panel includes simulated organic carbon aerosol.

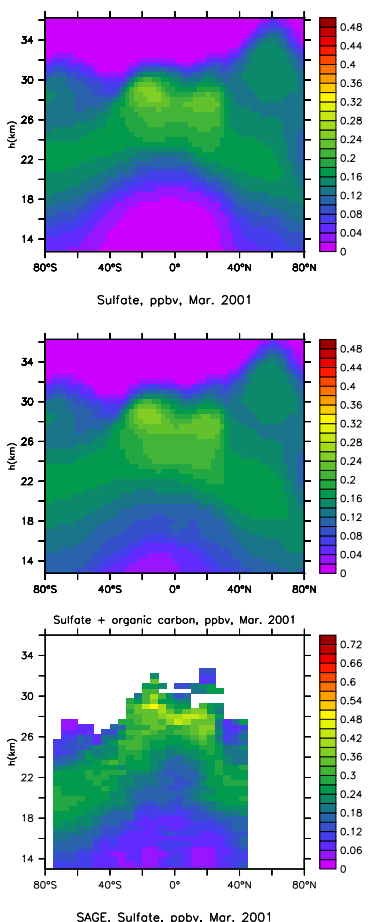


Fig. 4. As Fig. 3 but for March 2001.

COS and
stratospheric aerosol

Brühl et al.

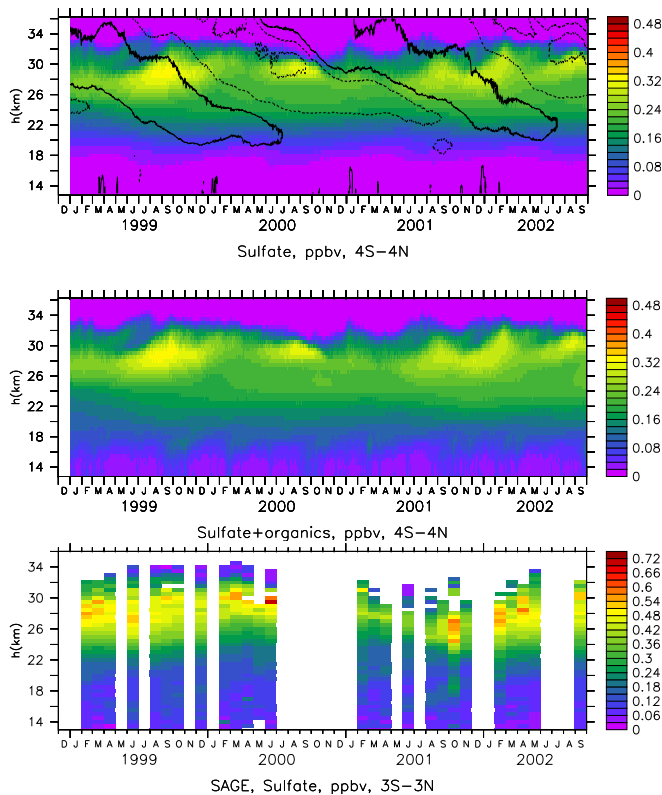


Fig. 5. Simulated (upper panel) and SAGE satellite derived (lower panel) sulphate aerosol in the tropics, ppbv. Black contours give the zonal wind (QBO), in steps of 20 m s^{-1} , beginning with -30 m s^{-1} . The middle panel includes simulated organic carbon aerosol.

[Title Page](#)[Abstract](#)[Introduction](#)[Conclusions](#)[References](#)[Tables](#)[Figures](#)[◀](#)[▶](#)[◀](#)[▶](#)[Back](#)[Close](#)[Full Screen / Esc](#)[Printer-friendly Version](#)[Interactive Discussion](#)

COS and
stratospheric aerosol

Brühl et al.

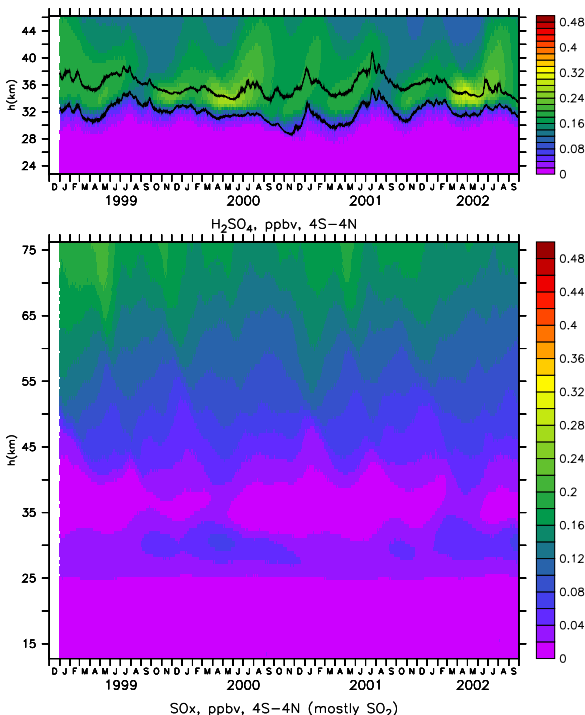


Fig. 6. Simulated gaseous H₂SO₄ and SO_x (mostly SO₂) in the tropics, ppbv. The contours in the upper panel show mean temperatures of 230 and 240 K, the region where sulphate aerosol evaporates.

[Title Page](#)[Abstract](#)[Introduction](#)[Conclusions](#)[References](#)[Tables](#)[Figures](#)[◀](#)[▶](#)[◀](#)[▶](#)[Back](#)[Close](#)[Full Screen / Esc](#)[Printer-friendly Version](#)[Interactive Discussion](#)

**COS and
stratospheric aerosol**

Brühl et al.

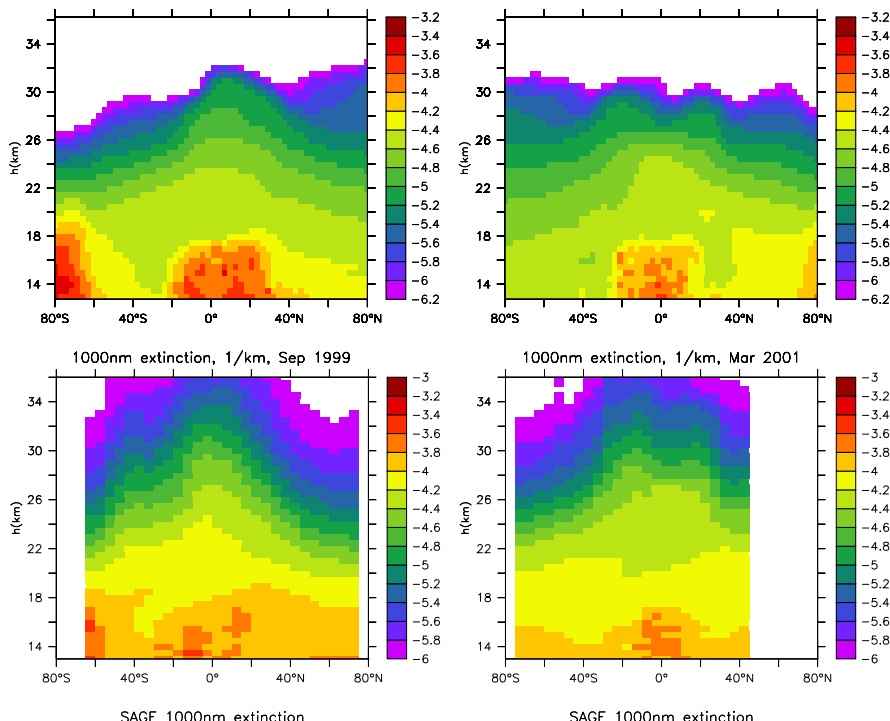


Fig. 7. Simulated (upper panels) and observed (lower panels) aerosol extinctions at 1000 nm (decadal logarithm) for September 1999 (left) and March 2001 (right).

[Title Page](#) [Abstract](#) [Introduction](#)
[Conclusions](#) [References](#) [Tables](#) [Figures](#)
[◀](#) [▶](#) [◀](#) [▶](#)
[Back](#) [Close](#) [Full Screen / Esc](#)

[Printer-friendly Version](#)
[Interactive Discussion](#)



COS and
stratospheric aerosol

Brühl et al.

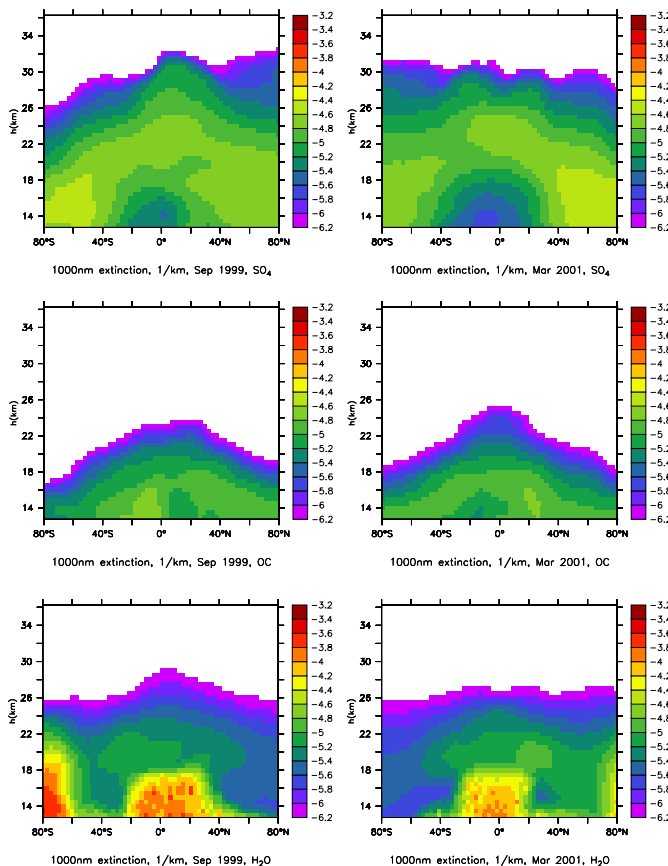


Fig. 8. Contribution of aerosol components to simulated total extinction (Fig. 7).

[Title Page](#)[Abstract](#)[Introduction](#)[Conclusions](#)[References](#)[Tables](#)[Figures](#)[|◀](#)[▶|](#)[◀](#)[▶](#)[Back](#)[Close](#)[Full Screen / Esc](#)[Printer-friendly Version](#)[Interactive Discussion](#)

COS and
stratospheric aerosol

Brühl et al.

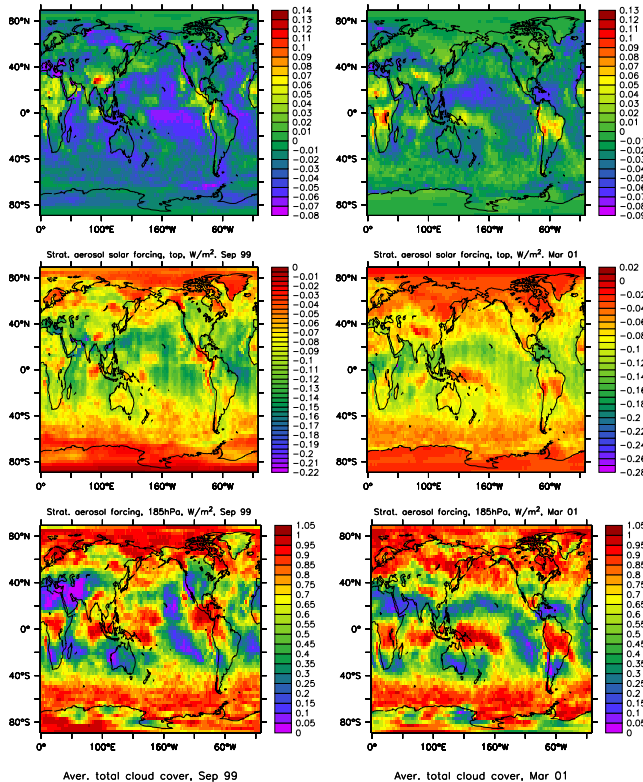


Fig. 9. Solar radiative forcing of stratospheric aerosol (above 110 hPa) at the top of the atmosphere (upper panels) and at 185 hPa (middle panels). The lower panels show the average total cloud cover.

[Title Page](#)[Abstract](#)[Introduction](#)[Conclusions](#)[References](#)[Tables](#)[Figures](#)[|◀](#)[▶|](#)[◀](#)[▶](#)[Back](#)[Close](#)[Full Screen / Esc](#)[Printer-friendly Version](#)[Interactive Discussion](#)